AN ACTION SPECTRUM APPARATUS

by

DONALD ELLIOTT BROOKS

B.Sc. (Hons.), University of British Columbia, 1964

A THESIS SUBMITTED IN PARTIAL FULFILMENT OF

THE REQUIREMENTS FOR THE DEGREE OF

MASTER OF SCIENCE

in the Department

of

PHYSICS

We accept this thesis as conforming

to the required standard

THE UNIVERSITY OF BRITISH COLUMBIA

April, 1967

In presenting this thesis in partial fulfilment of the requirements for an advanced degree at the University of British Columbia, I agree that the Library shall make it freely available for reference and study. I further agree that permission for extensive copying of this thesis for scholarly purposes may be granted by the Head of my Department or by his representatives. It is understood that copying or publication of this thesis for financial gain shall not be allowed without my written permission.

Department of ___Physics___

The University of British Columbia,
Vancouver 8, Canada

Date ___April 25, 1967___

ABSTRACT

An instrument is described which is capable of measuring the action spectrum of the removal of CO inhibition of respiration by light. In the method employed here, a cell suspension in a $CO-O_2$ atmosphere is alternately exposed to two wavelengths of light. Their photochemical effects are balanced using an O_2 electrode as the null detector. The light intensities at the balance points from a series of wavelength pairs are used to determine the ratios of the extinction coefficients of the CO - oxidase complex, at the various wavelengths, to the extinction coefficient at a standard wavelength. An action spectrum for Bakers yeast is shown.

ACKNOWLEDGMENTS

TABLE OF CONTENTS

LIST OF FIGURES

LIST OF TABLES

Introduction

An action spectrum is a representation of some biological activity which varies as a function of the wavelength of light incident on the organism under observation. If some measure of the activity being monitored is plotted as a function of the wavelength of light incident on the sample, the resulting graph (the action spectrum) will characterize the absorbing species controlling the action (1,2). The action that the present apparatus is designed to characterize is the light sensitive inhibition of respiration by carbon monoxide.

Warburg and his coworkers developed the classical manometric technique for this measurement (3). A more sensitive apparatus designed to make the same measurement, using polarography, was later developed by Castor and Chance (4). This thesis describes in detail an action spectrum apparatus based on their instrument.

Chapter I outlines the theoretical background of the method, discusses the conditions necessary for an action spectrum measurement of this type, and describes in broad outline the measuring procedure. Chapters II, III, and IV describe in detail the various parts of the apparatus, the design considerations which led to their use, and their application in the measuring system. The calibration, operation, and performance of the instrument in measuring an oxidase action spectrum is discussed in Chapter V. Chapter VI offers some suggestions for improvements in, and extensions to, the apparatus as it now exists.

CHAPTER I

The Theory and Application of
the Action Spectrum Method

I-1. Theoretical Background

    1.1 Problems to which Action Spectrum Methods are Suited

        In principle, an action spectrum may be taken of any bio-
logical activity which is linked to the absorption of specific wavelengths
of light. The method has two advantages over absorption spectrophotometry:

        (i)   a spectrum can be obtained when there are too

few molecules to provide measurable absorption;

        (ii)   the spectrum characterizes the molecule or

molecules which are biologically functional in the

process being observed.

Thus, under the conditions to be described, relative extinction coefficients
may be determined for compounds which cannot be extracted in an examinable
form, or whose absorption bands may be masked by the absorption bands of
other cell constituents. Primarily, however, the method is used to deter-
mine the active molecule or molecules in biological action affected by
light.

    1.2 The CO-Oxidase Action Spectrum

        Biophysical and biochemical evidence gives some of the
chemistry and mechanism of respiration and its light sensitive inhibition
by CO. (3) Based on such evidence, a set of chemical equations may be
set up representing the combination of the enzymic iron in the cellular
electron transport system with either oxygen or carbon monoxide. In the
equations and kinetic analysis that follow, $k_{1 \to 5}$ are reaction velocity

constants which are independent of light intensity, and k_λ is the reaction velocity constant of the light induced breakdown of the $Fe''-CO$[1] complex at a wavelength λ. The analysis investigates the steady-state behaviour of the system when irradiated by monochromatic light of any chosen wavelength, and shows how one can calculate the relative extinction of the $Fe''-CO$ complex at each wavelength. The relative extinction coefficient is the ratio $\epsilon_\lambda / \epsilon_s$, where s represents a chosen standard wavelength.

The stoichiometric equations are:

$$Fe'' + O_2 \underset{k_2}{\overset{k_1}{\rightleftharpoons}} Fe''-O_2 \overset{k_5}{\longrightarrow} Products \qquad (I-1)$$

$$Fe'' + CO \underset{k_4}{\overset{k_3}{\rightleftharpoons}} Fe''-CO \quad k_\lambda \qquad (I-2)$$

Let:

$(e-p-q) = [Fe'']$ $\qquad$ $p = [Fe''-O_2]$

$x = [O_2]$ $\qquad\qquad$ $q = [Fe''-CO]$

$y = [CO]$

Then, it follows from the law of Mass Action, that:

$$\dot{p} = k_1 x (e-p-q) - (k_2 + k_5) p \qquad (I-3)$$

$$\dot{q} = k_3 y (e-p-q) - (k_4 + k_\lambda) q \qquad (I-4)$$

The respiration rate, $-\dot{x}$, is given by:

$$-\dot{x} = \dot{p} + k_5 p$$

---

1. $Fe''-CO$ is the abbreviation for the complex formed by the carbon monoxide and the reduced heme iron of the enzyme.

In a steady state:

$$\dot{q} = 0$$
$$\dot{p} = 0 \quad \text{which implies} \quad -\dot{x} = k_5 p$$

and therefore the respiration rate is directly proportional to p. So, solving for p in (I-1) and (I-2):

$$p = \frac{e}{1 + \dfrac{K_m}{x} + \dfrac{K_m\, y}{K_y\, x}}$$

where:
$$K_m = \frac{k_2 + k_5}{k_1} \quad , \quad K_y = \frac{k_4 + k_\lambda}{k_3}$$

$$\therefore \quad \frac{e}{p} = 1 + \frac{K_m}{x} + \frac{K_m\, y}{K_y\, x}$$

Let $p = p_0$ be the concentration of $Fe''-O_2$ when no CO is present ($y = 0$). Then $\dfrac{e}{p_0} = 1 + \dfrac{K_m}{x}$, and substituting back gives:

$$\frac{K_m\, y}{e\, x} = K_y \left[\frac{1}{p} - \frac{1}{p_0} \right] \qquad (I\text{-}5)$$

If x and y remain constant, the left hand side of (I-5) is a constant. Changing the wavelength or intensity of light incident on the reacting species will affect only p, and K_y, through k_λ. So, at wavelengths λ_1 and λ_2, if the respiration rates, and thus the values of p, are equal: $K_{y_1} = K_{y_2}$ which implies $k_{\lambda_1} = k_{\lambda_2}$. These reaction velocity constants are related to the extinction coefficients of the $Fe''-CO$ complex, as shown below.

Consider a layer of suspended absorbing molecules of thickness d containing a reacting species at a concentration c. Let a monochromatic beam of wavelength λ and quantum intensity J_λ illuminate an area A of the solution, and let the extinction coefficients of the

reacting species be β . Assume that d and c are such that a negligible number of quanta are absorbed, so that all absorbing centers are exposed to equal intensities. Then, the number of mole quanta absorbed per second is given by $\beta J_\lambda c A d$. The number of moles per second reacting as a result of the light energy absorbed will be:

$$-\dot{c} A d = \phi \beta J_\lambda c A d$$

where ϕ is the photochemical yield, defined as the ratio of the number of molecules reacting, to the number of quanta absorbed. Thus

$$-\dot{c} = \phi \beta J_\lambda c$$

and the reaction velocity constant, defined by $k_\lambda = \dfrac{-\dot{c}}{c}$ is given as:

$$k_\lambda = \phi \beta J_\lambda$$

Converting the quantum intensity to energy units, and writing $\epsilon = \dfrac{\beta}{2.303}$ as the extinction coefficient based on the common logarithms:

$$k_\lambda = \frac{\phi \epsilon_\lambda W_\lambda \lambda}{2.303 N_o h c'} \qquad (I-6)$$

where: W_λ = intensity in energy units

N_o = Avogadro's number

h = Planck's constant

c' = speed of light

Warburg and others (3,5) have shown that for a number of heme - CO complexes in different molecules, ϕ is independent of wavelength. Thus, under the conditions for which (I-6) applies:

$$\epsilon_{\lambda_1} W_{\lambda_1} \lambda_1 = \epsilon_{\lambda_2} W_{\lambda_2} \lambda_2$$

$$\frac{\epsilon_{\lambda_1}}{\epsilon_{\lambda_2}} = \frac{W_{\lambda_2} \lambda_2}{W_{\lambda_1} \lambda_1} \qquad (I-7)$$

I-2. Generalization of the Kinetics

The chemical equations I-1 and I-2 seem to be a reasonable representation of the light sensitive inhibition of respiration by CO. Explicit knowledge of the reaction constants and concentrations would be necessary if the extinction coefficients of the enzyme - CO complex were to be calculated absolutely. However, the relative values $\epsilon_\lambda / \epsilon_{550}$, do not depend on the kinetic analysis for their validity. If changing from quantum intensities J_{λ_1} to J_{λ_2} leaves the system chemically and kinetically unchanged, one need logically assume only that the product $\phi \beta J$ is constant between the two intensities. No further details of the biological action need be known.

I-3. Necessary Conditions for Determining an Oxidase Action Spectrum

The use of the action spectrum method in oxidase identification depends on the following:

(i)   the iron containing enzyme reacts with oxygen

(ii)   the iron containing enzyme also binds carbon monoxide

(iii) the oxygen concentration controls the respiration rate

(iv)   the oxygen and carbon monoxide compete for the binding site on the enzyme.

I-4. General Outline of the Method

In the apparatus to be described, the measurement of the photochemical effect of a wavelength λ was made by alternately illuminating the reaction solution with a narrow bandwidth monochromatic beam and

a comparison beam of fixed spectral composition and variable intensity. The intensity of the comparison beam was adjusted until the respiration rate sensor indicated no change when the beams were alternated. This procedure was carried out at all wavelengths for which the relative extinction coefficients were measured. The block diagram of the measurement apparatus is shown in Figure 1.

The extinction coefficients, relative to that at $\lambda = 550$ nm, were calculated from the expression:

$$\frac{\epsilon_\lambda}{\epsilon_{550}} = \frac{C_\lambda \; W_{550} \; 550}{W_\lambda \; C_{550} \; \lambda} \tag{I-8}$$

which follows directly from equation I-7. In (I-8):

C_λ = intensity of comparison light which gives same photochemical effect as λ

C_{550} = intensity of comparison light which gives same photochemical effect as 550 nm.

Electrode Current Msmt.

Light Intensity Msmt.

Phase Sensitive Detector

Ref. Electrode

PbS Detector

Monochromatic or Comparison Beam

Oxygen Electrode

Cell Suspension

Cone Channel Condenser

Barrier layer cell for ref. signal

Synch. Motor

110 v. Mains

Stabilized Light Source

Chopper

Monochromator

FIGURE 1-A

Block Diagram of Apparatus

Exit Slit

Diffraction Grating

Exit beam either monochromatic or white comparison light

Plane mirror slides into white beam to produce comparison beam

Monochromatic

Entrance Slit

Micrometer head sets louver angle

Entrance beam white light from tungsten lamp

White

Louvers set intensity of comparison beam

Plane mirror replaces grating in comparison beam

Concave mirror
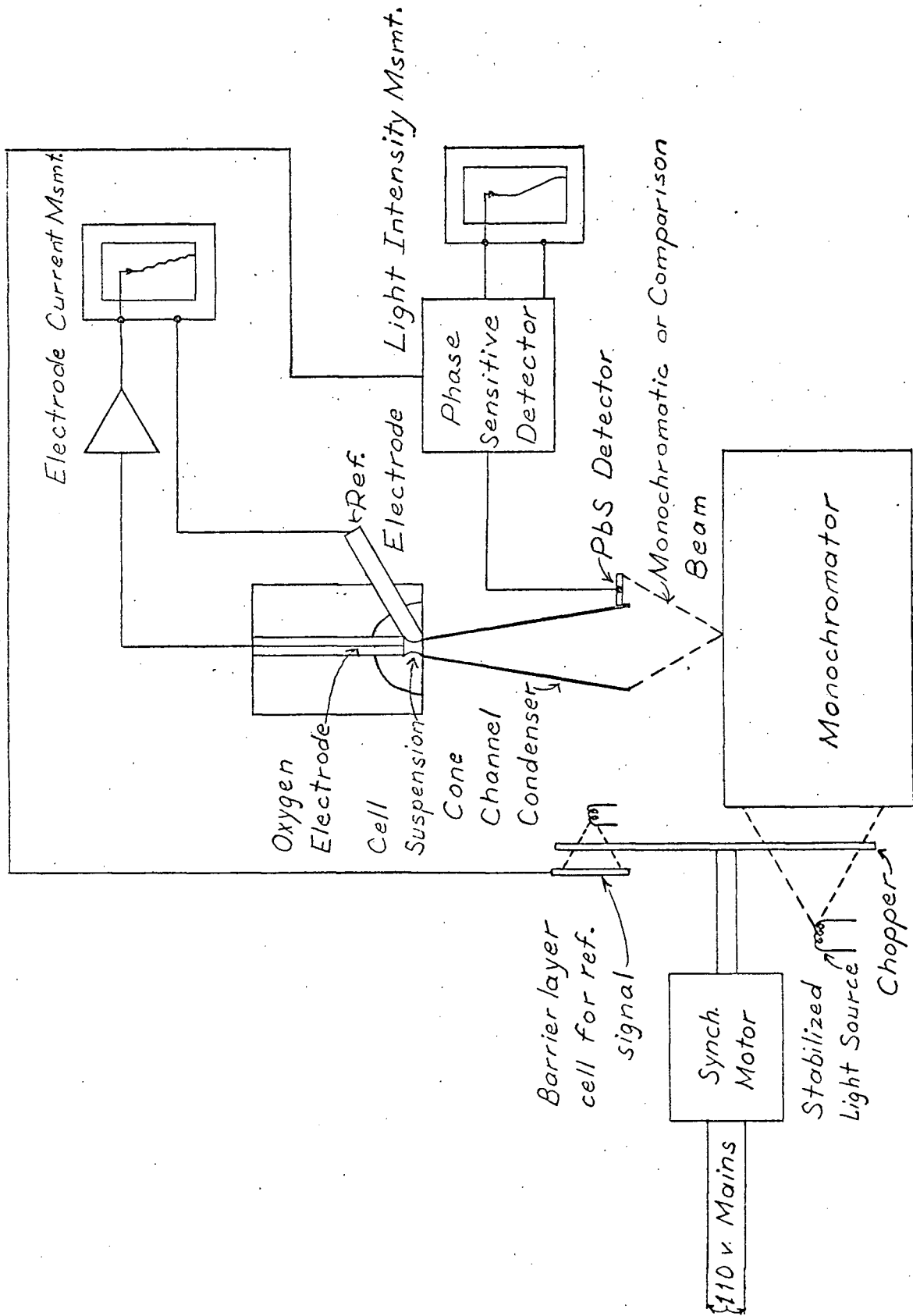
FIGURE 1-B
Optical Path Inside Monochromator

CHAPTER II

Optical System

II-1. The Monochromator and its Modifications

Any apparatus designed to take an action spectrum requires
a source of monochromatic light of variable wavelength, and an optical
system to deliver the light to the biological sample. In the present
apparatus, the monochromatic light is supplied by a Bausch and Lomb Grating
Monochromator employing a diffraction grating 50 mm x 50 mm ruled at
600 grooves/mm. The instrument has a linear dispersion of 6.6 nm/mm at the
exit slit. Quartz condensers image the light from the source on the en-
trance slit which lies in the focal plane of a front surfaced concave
mirror of focal length 250 mm. The collimated beam from this mirror is
reflected to the grating, dispersed back to the concave mirror, condensed,
and imaged at the exit slit. Wave length selection at the exit slit is made
by rotating the grating about a vertical axis, thus scanning the dispersed
beam across the exit slit. Wavelengths from 200 nm to 1,400 nm in the
first order are available, although above 400 nm the second order begins
to overlap, impairing the purity of the beam. The width of the slit deter-
mines the bandwidth of the monochromatic light passed. Optimum purity and
intensity for a given slit width are obtained when the exit and entrance
slits are set equal.

Since the apparatus is designed for initial use between
350 nm and 1,000 nm, a glass envelope bulb is used. The bulb is rated at
8 v - 50 w, is of Japanese make (commercial name: "Astron" or "Ace"), and
is housed in a water cooled jacket. It is run from a 10 v - 100 w Sorensen

DC power supply stabilized to $\pm$ 0.25%. The filament is surrounded by a glass bulb covered everywhere inside with a reflective coating except where the beam emerges. The bulb thus acts as a spherical mirror to the part of the radiant energy that would normally be lost from the system. The added reflected light greatly increases the intensity available at the quartz condensing lenses of the monochromator, although the collimation caused by the mirror causes some defocussing at the grating.

The action spectrum method used here requires that a beam of fixed spectral content be alternated on the sample with the monochromatic light of variable wavelength. The fixed comparison beam must be of variable intensity but must not contain an appreciable amount of infra-red radiation. Unless such radiation is filtered out, both thermal damage to the biological sample, and thermal instabilities in the electrode current may occur. The comparison beam light is introduced by placing a plane front surfaced mirror in the white beam between the concave mirror and the diffraction grating. This beam is reflected to the floor of the monochromator box, where another plane mirror reflects the light back to the first mirror, then to the concave mirror, which focusses it on the exit slit. The arrangement is such that, as nearly as possible, the second plane mirror and the diffraction grating are in optically equivalent positions. A series of parallel louvers mounted above the second plane mirror acts as the intensity control. The louvers are ganged together, and their angular position with respect to the beam determines how much of the light is reflected to the exit slit. The louver angle is controlled by a micrometer head, mounted in the side of the monochromator box. It screws against a spring loaded arm to which the hinged louvers are attached. There is a provision for mounting filters

above the set of louvers to limit the spectral content of the comparison
light, but it was found that locating the filters in this position intro-
duces a great deal of scattered light into the system. Instead, the filters
are placed outside the monochromator box, between the quartz condensing
lenses and the entrance slit.

The change between the monochromatic and comparison beams is
made by mechanically inserting the first plane mirror into the white beam
from the concave mirror. The second mirror, intensity controlling louvers,
and filter holder, are all out of the normal optical path and remain
stationary throughout the change. The first mirror runs on a track, the
position on which is controlled by a lever arm external to the box. Mech-
anically linked to this arm are two filter holders, one of which introduces
an infra-red filter into the optical path when the comparison light is
illuminating the sample, but is not in the path when the monochromatic
light is being used. The second holder is inserted into the optical path
only when the sample is monochromatically illuminated. This second holder
is used primarily for broad band filters which eliminate interference from
the second and third orders in the monochromatic beam.

II-2. Cone Channel Condenser

2.1 Design Considerations

In order to produce a light intensity at the biological
sample high enough to get measurable effects even with the most insensitive
enzymes, the exit beam from the monochromator must be concentrated in some
way. Also, since the lamp filament is focussed at the exit slit, the
intensity will vary across the slit and some scrambling of the beam will
be necessary to get an even distribution throughout the drop, particularly

in the comparison beam. This is important, since the distribution of comparison and monochromatic beams must be proportional throughout the drop to avoid transient effects when the beams are interchanged. Further, the more even the illumination on the individual cells, the more closely the assumptions will apply under which (I-6) was derived. A quartz achromatic lens system, as well as being expensive, does not provide such a diffuse beam, even when filtered. A better system is provided by a cone channel condenser, a modification of the device described by Williamson (6). The condenser used is a four sided pyramid of square cross-section open at both ends. The inner surfaces are front surfaced mirrors. The base opening is 11 mm square and sits on the exit slit of the monochromator. The top is 1.6 mm square and fits flush up against the cover slip forming the bottom of the electrode chamber. The condenser is designed to produce an even intensity distribution over a complete hemispherical solid angle of 2π at the exit of the cone, as well as increase the intensity at the exit over that at the base. The cone is designed so that the most widely divergent ray of the entrance beam to the cone suffers multiple internal reflections until it emerges at 90° to the optic axis of the condenser. Less divergent rays entering suffer fewer reflections and emerge at smaller angles to the axis. The length of the cone that will give such reflections is critical. It is determined by analyzing a ray tracing diagram showing the optical path of the extreme ray from the monochromator entering the condenser.

The diagram is constructed as shown below in Figure 2. The cone is drawn on the optic axis, and the extreme ray from the monochromator is drawn at an angle V to the axis, entering the mouth of the cone.

Instead of tracing the path of the ray through its reflections, every time
the ray reaches a reflecting surface the cone is drawn as being reflected
about that surface. Thus, the extreme ray will appear as a straight line
on the diagram, while the cone ends and their reflections will form two
concentric polygons. As long as the cone angle is small, the inner polygon
may be replaced by a circle as shown in the diagram, and the outer circle
may be excluded during the analysis. If the extreme ray cuts this inner
circle, the ray will emerge from the end of the cone at the angle the ray
makes with the circle at that point. For the ray to emerge at 90° to the
cone, it must lie tangent to the circle, as shown. The length of the cone,
x, is the distance between the mouth, of width 2s, and the circle. The cone
angle, β , is that angle at the centre of the circle formed by the radius
continuous with the cone edge.
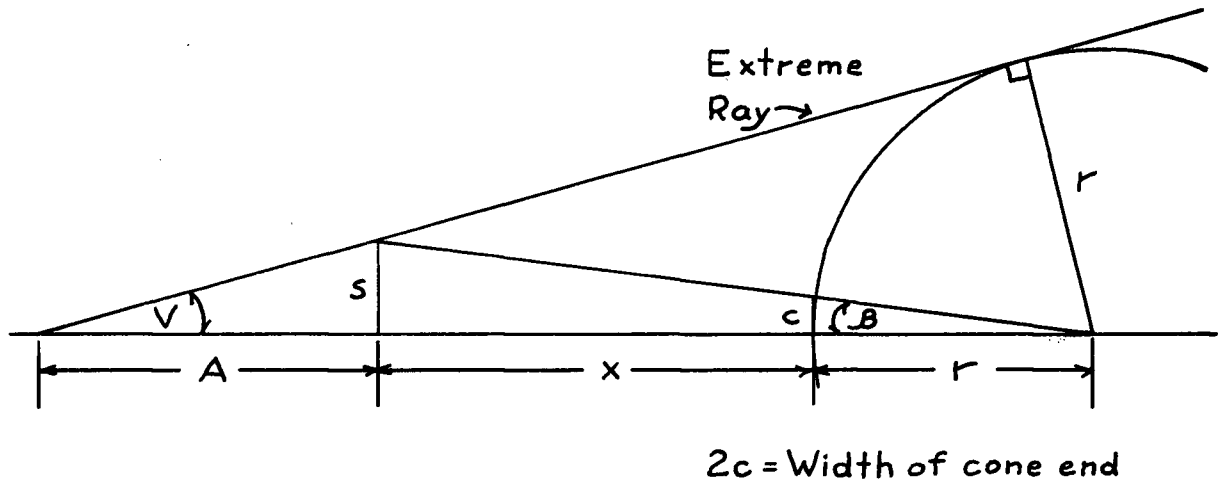
Figure 2

Ray Tracing Diagram for Condenser Design

The length $x = x(c,s,V)$ is found from:

(i) $\cotan \beta = \dfrac{x+r}{s} = \dfrac{r}{c} \Rightarrow r = \dfrac{cx}{s-c}$

(ii) $A = s \cotan V$

(iii) $r = (A+x+r) \sin V \Rightarrow r = \dfrac{\sin V (s \cotan V + x)}{1 - \sin V}$

Eliminating r and A from these three equations, and solving for x gives:

$$x = \dfrac{(s-c) \cos V}{c/s - \sin V}$$

In the Bausch and Lomb monochromator, the angle V is determined by the aperture stop, which in this instrument is the grating area, and the focal length of the condensing concave mirror. Thus:

$$\tan V = \dfrac{25\,mm}{250\,mm}$$

$$\therefore V = 5°43'$$

The exit slit length = 2s = 11 mm and the cone end width 2c was taken as 1.8 mm. These figures give: x = 102 mm.

2.2 Construction of the Cone Channel Condenser

The cone was constructed from glass strips of appropriate shape, ground flat on one edge (obtained from Emerald Glass Co., Toronto, Ont.). They were placed two at a time in a jig which supported them at the ends, and held them at right angles with one ground edge butted up against the surface of the other piece. The glass was held in this position with setting screws which determine the angle, and the size of the two end openings. The jig was then hung in an evacuated chamber and aluminum evaporated onto the inner surfaces of the two pieces. All setting and holding of the glass had to be mechanical up to this point, since epoxy or other glues evaporated too rapidly when the pressure was reduced in the chamber,

and the vacuum obtainable was insufficient to allow good aluminum evaporation. Once aluminized, the two pieces were glued with epoxy on the back of the joint. Two such assemblies were then placed vertically in another jig whose base and top were of proper size to set the base pieces in an 11 mm square and the top of the cone in a 1.6 mm square. These two units were also epoxied on the back of the joint to form the cone. Some adjustment to the length could have been made by coating the aluminized surface with paraffin, grinding the glass down, then removing the paraffin by setting the cone in hot water.

Unfortunately, an error in the calculation of the extreme ray angle from the monochromator in the original cone design resulted in the cone being built 111 mm long. This longer length caused some loss in intensity at the sample. However, even with the low power light source used, ample intensity was available at the end of the cone when slip widths of the order of 0.5 mm were used.

CHAPTER III

Measurement of Light Intensity

III-1. General Design Requirements for the Detector

The determination of an action spectrum requires an accurate, reproducible measure of light intensity. The light detector in the apparatus must have a high signal to noise ratio, it must be able to efficiently detect radiation of wavelengths from 200 nm to 1,000 nm, and it should preferably be of small enough size to be introduced easily into the optical system employed in the apparatus. The relative cost of the detection system is also an important consideration.

III-2. Comparison of Types of Detectors

2.1 Terms of Comparison

A quantitative comparison of the various types of light detectors available has been made by Jones (7). He considers them in terms of their detectivity. The detectivity is the ratio of the gain of the detector, that is the number of volts delivered by the detector for every watt of incident radiant power, to the r.m.s. noise voltage introduced into the output by the detector itself. Since the response of the device will in general vary with the frequency at which the light beam is modulated, the detectivity, D (f), will be a function of the modulation frequency f. Thus:

$$D(f) = \frac{R(f)}{r.m.s.\ noise}$$

(III-1)

where R (f) = responsivity, the ratio of the detector output in volts to

the radiant power input, in watts. If the noise voltage is decomposed into spectral components at frequency f, W (f), such that the mean square noise voltage $\overline{n^2}$ is given by:

$$\overline{n^2} = \int_0^\infty W(f)\,df \qquad\qquad \text{(III-2)}$$

then the detectivity over a unit bandwidth of noise centered on a frequency f is defined by:

$$D_1(f) = \frac{R(f)}{[W(f)]^{1/2}} \qquad\qquad \text{(III-3)}$$

Further, a time constant, τ , which is a measure of the response time of the detector, may in general be defined by:

$$\tau = \frac{D_1(f_m)^2}{4\int_0^\infty D_1(f)\,df} \qquad\qquad \text{(III-4)}$$

where f_m is the modulation frequency which maximizes $D_1(f)$. In many types of detectors, the responsivity spectrum is characterized by the time constant in the form:

$$R(f) = \frac{R_{max}}{[1 + (2\pi f \tau_p)^2]^{1/2}} \qquad\qquad \text{(III-5)}$$

where R_{max} is the particular detector's maximum responsivity, and τ_p is its time constant.

Detectors are classified more generally by Jones into Class I or II. Since D (f) is found to depend upon both τ and the sensitive area A in either of two ways, this fact is made the basis of the classification:

$$\text{Class I} \qquad D = k_1 \left[\frac{\tau}{A}\right]^{1/2}$$

Class II $D = k_2 \dfrac{\tau}{A^{1/2}}$

where k_1 and k_2 are constants. In order to more easily compare detectors within a given class, their detectivities are compared to the detectivity of the hypothetically "ideal" detector of the class. The value of the fraction thus formed is termed the figure of merit of the detector. The ideal Class I detector is taken to be a perfectly black thermal detector whose output is limited by only photon noise. If the detector and the noise it produces both have the same bandwidth its detectivity is given by

$$
\begin{aligned}
D_P &= \frac{1}{(4\sigma k T^5)^{1/2}} \left[\frac{\tau}{A} \right]^{1/2} \\
&= 3.62 \times 10^{10} \left[\frac{\tau}{A} \right]^{1/2}
\end{aligned}
\qquad \text{(III-6)}
$$

thus the Class I figure of merit, M_1, is given by

$$
M_1 = \frac{D}{D_P} = 2.76 \times 10^{-11} D \left[\frac{A}{\tau} \right]^{1/2}
\qquad \text{(III-7)}
$$

Detectivities in Class II are related to the theoretical upper limit for thermocouples and bolometers, estimated to be

$$
D_H = 0.33 \times 10^{11} \frac{\tau}{A^{1/2}}
\qquad \text{(III-8)}
$$

Therefore the figure of merit, M_2, is given by

$$
M_2 = 3 \times 10^{-11} \frac{D A^{1/2}}{\tau}
\qquad \text{(III-8)}
$$

2.2 Types of Detectors Under Consideration

The types of detectors considered for use in the action spectrum apparatus were thermal detectors, photoemissive detectors, and photoconductive cells.

2.21 Thermal Detectors

Thermal detectors operate by converting radiation power

into a voltage by means of a temperature change in the absorbing element. An important parameter in their performance is the physical time constant, $\tau_\rho = {}^C\!/K$, where

        C = thermal capacity per unit sensitive area

        K = conductivity per unit area.

These thermal detectors are of three types:

    (i)   Thermocouples:

        The theoretical figure of merit of a Johnson noise limited thermocouple is given by

$$M_\lambda = \frac{3\times10^{-11}\,\epsilon\,S}{(kT^2C)(L_1^{1/2}+L_2^{1/2})} \qquad \text{(III-9)}$$

where: ϵ = emissivity of receiver

        S = thermoelectric power of pair of metals

        k = Boltzman's constant

        T = absolute temperature

        C = thermal capacity of receiver per unit area

$L_{1,2} = \lambda^* \rho / T$ for thermocouple wires 1 and 2, where λ^* = thermal conductivity, ρ = electrical resistivity. The highest figures of merit thus far obtained for thermocouples are about 1.0, while the Eppley thermopile is quoted in Jones (7) as having a figure of merit of approximately 0.025, and a time constant of the order of 2 seconds.

(ii) Radiation Bolometers:

        These are essentially resistance thermometers. Radiation heats a ribbon through which a steady current flows, changing its resistance. The highest figure of

merit obtained at room temperature for these detectors is about 0.5.

(iii) Golay Pneumatic Heat Detector:

The Golay detector is a gas-filled chamber with an infra-red transmitting front window. A low heat capacity metallized membrane absorbs the incident radiation and increases in temperature, exchanging heat to the gas. The gas pressure increases and deforms a flexible membrane which causes a reflected beam to deflect as a measure of the radiation absorbed. The Golay deviates from an ideal Class I detector only in that there is some absorption in the entrance window, the heat absorbing membrane is not perfectly black, and there is some conduction from this membrane to the walls of the chamber. The combination gives a figure of merit of $M_1 = 0.275$.

2.22 Photoemissive Detectors

Photoemissive detectors employ the photoelectric effect to detect radiation intensities. The secondary electrons emitted are accelerated through a potential difference and measured as a cathode current. This current is either measured immediately, as in a vacuum phototube, or after internal amplification by a cascade process either in a gas (gas phototube) or between members of a series of dynodes in a high field gradient (photomultiplier). By far the most efficient of these three is the photomultiplier, since it supplies essentially noisefree amplification with gains of the order of 10^5. The figure of merit of a photomultiplier operating in the visible region, for instance, (the photoemissive surface type is designated

S-4 for this region of spectral response) has a figure of merit, $M_1 = 140,000$.
An S-5 photomultiplier, operating in the ultraviolet and visible has
$M_1 = 12,700$. The figures of merit of gas phototubes and non-amplifying
phototubes are several orders of magnitude lower, all having M_1 100.

Photomultipliers do, however, have several disadvantages.
The accelerating potentials in the tubes are of the order of kilovolts,
and must be highly stabilized. Thus, extremely well regulated high voltage
power supplies are needed to run the photomultipliers, and their cost is
high. The tubes often exhibit some gain instability over a period of time.
While the sensitive areas may be small, the over-all tube size is quite
large, and the measuring system as a whole is rather bulky and awkward to
mount, particularly in the optical system used in the action spectrum
apparatus. More important, no one photomultiplier gives useful detection
over the wavelength range required, so different tubes would have to be
employed over different spectral regions. Thus, photomultipliers would
not seem to fulfil adequately the requirements of the apparatus.

2.23 Photoconductive Cells

Photoconductive cells are solid state devices which produce
useful detectivities in the ultraviolet, visible, and infra-red regions of
the spectrum. It is believed that the light quanta incident on the detector
raise electrons from the ground band or impurity centers into the conduction
band of the solid, thus decreasing the resistance of the detector. The
increase in current may be monitored as a measure of the radiation intensity.

The Kodak Ektron Detectors, made of either lead sulphide or
lead selenide deposited on glass, are typical photoconducting cells. They
will usefully detect radiation between 200 nm and 5,000 nm with time

constants between 2 and 1,000 microseconds. Their detectivities, normalized to unit area and bandwidth as given in the technical pamphlet "Kodak Ektron Detectors for the Infrared" (1960) are between 10^{10} and 10^{11}. This data gives, for the detectivity of highest responsivity, a detectivity of 3.5×10^{10} at 600 nm. Taking the value of the time constant to be the upper advertised limit of 1×10^{-3} sec. which applies for the detectors of highest detectivity, and an area of 0.04 cm^2, the figure of merit M_1 calculated from (III-7) is $M_1 \approx 6$. This value is lower than those for photo-tubes and photomultipliers, but at least six times higher than those for thermal detectors.

One disadvantage of the lead sulphide detector is a significant temperature dependence of both the signal and the signal to noise ratio. The Kodak Ektron Detector handbook provides the semi-lot plot of signal versus temperature shown in Figure 3. Calculation of the slope of the graph gives:

$$\alpha = \frac{1.0}{-43.5 \pm 1.0 \,^{\circ}c} = -2.3 \times 10^{-2} \pm 2\% \ deg^{-1}$$

The temperature dependence of the output of the lead sulphide cell, and hence of any signal S proportional to it, is then given by:

$$\Delta(\log S) = (-2.3 \times 10^{-2} \pm 2\%) \Delta T \qquad \text{(III-10)}$$

The advantages of the solid state device, however, outweigh its disadvantages. Lead sulphide cells may be constructed with virtually any shape and size of sensitive area; typically of the order of 1 to 20 mm square. The power necessary to operate the detector is supplied by an inexpensive 22.5 volt battery, allowing complete electrical isolation from the rest of the electronics in the apparatus. Further, the entire system
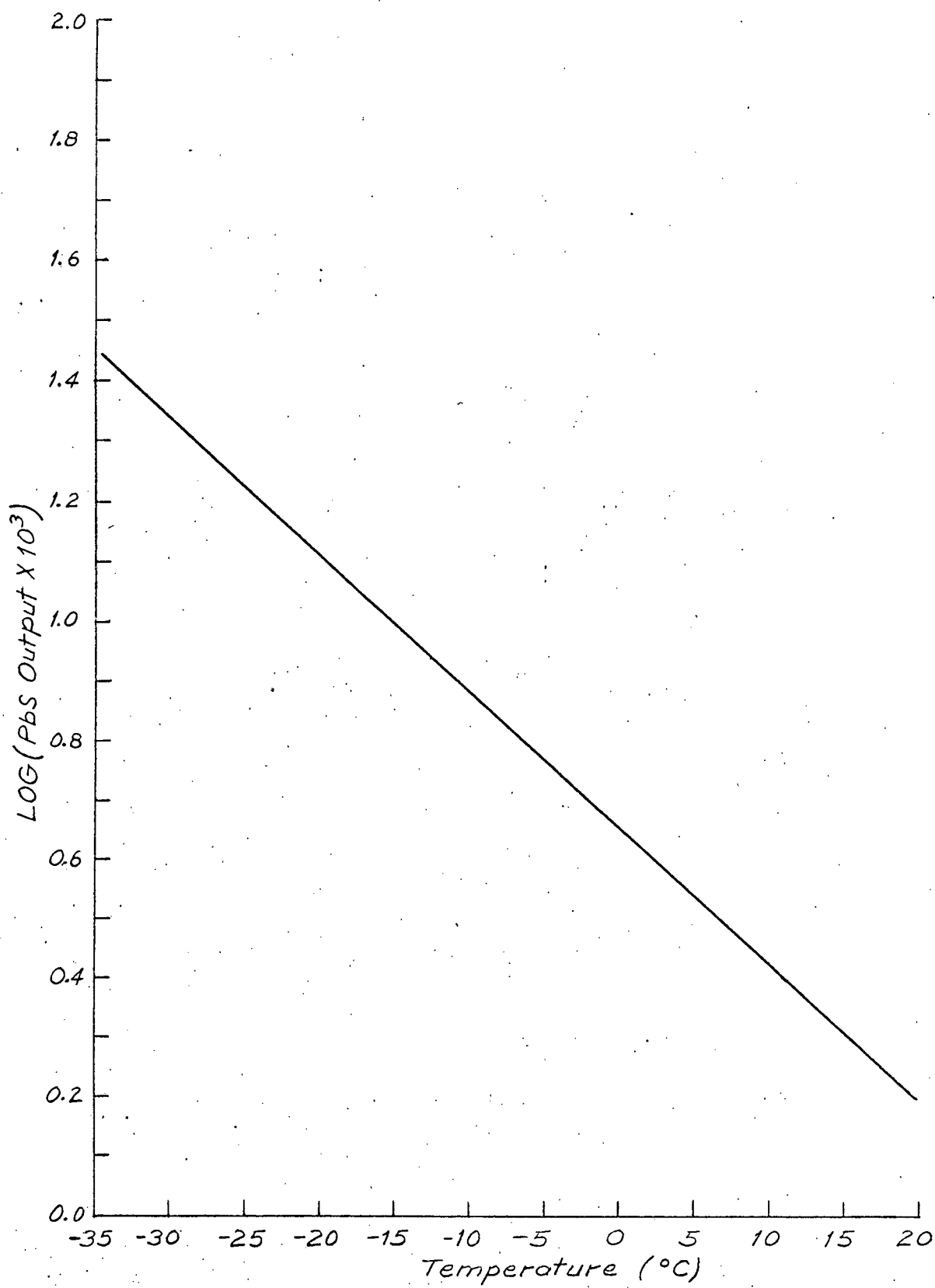
FIGURE 3

Semi-log Plot of PbS Output vs Temperature

is physically compact and easy to mount. Thus, on the basis of its figure
of merit, broad wavelength sensitivity, small size and low cost, it was
decided to use a lead sulphide cell as the radiation intensity detector in
the action spectrum apparatus.

III-3. Light Intensity Measurements in the Apparatus

3.1 Sampling the Beam for Intensity Measurements

In operation, two PbS cells are wired in series with a
22.5 v battery. One of the cells is exposed to the radiation to be measured,
and the other is masked to act as a load resistor across which the voltage
changes, proportional to the light intensity, appear. A masked PbS detector
is used as the load resistor because its resistance will be affected by
humidity, temperature, applied voltage and other external conditions in
the same way as that of the PbS cell actually detecting the radiation.
Thus the voltage changes actually measured should be proportional to the
true values of intensities incident on the exposed cell. Unfortunately,
this matching only holds if the two detectors are equally illuminated, since
the temperature dependence of the resistance in the photoconducting state
differs from that in the dark, giving rise to the expression (III-10).
The temperature dependence would be much greater if an ordinary resistor
were used as the load resistor.

The PbS cell employed in the apparatus has a sensitive area
2 mm x 2 mm covered by a quartz cover slip. It is mounted at the end of
the exit slit of the monochromator, adjacent to the base of the cone channel
condenser as shown in Figure 4. The light beam sufficiently fills the slit
that an appreciable amount is available for the intensity measurement
outside the cone. By sampling the beam outside the cone, none of the

Cone channel
condenser

Mercury
thermometer

Wakefield
Thermal Cmpd.

Leads from
detectors to PbS
polarizing cct.

Monochromator
slit, length = 20mm

Light beam

Back to back
PbS detectors

Front surfaced mirror
reflects part of beam
onto sensitive area of
PbS detector

30 v.

PbS cell
exposed
to beam

Output

330K   69K
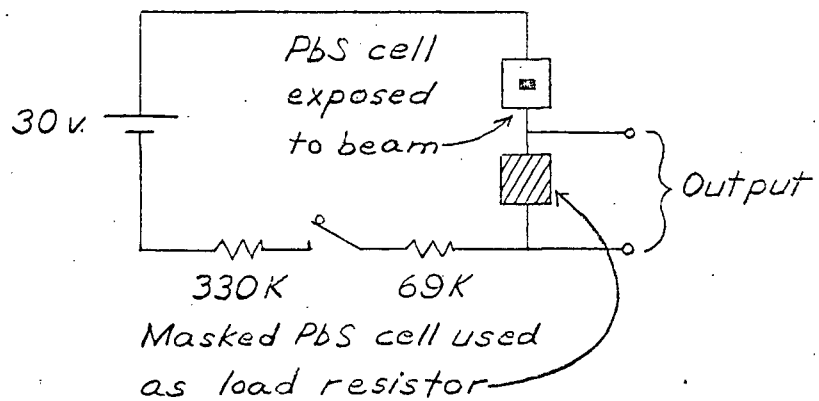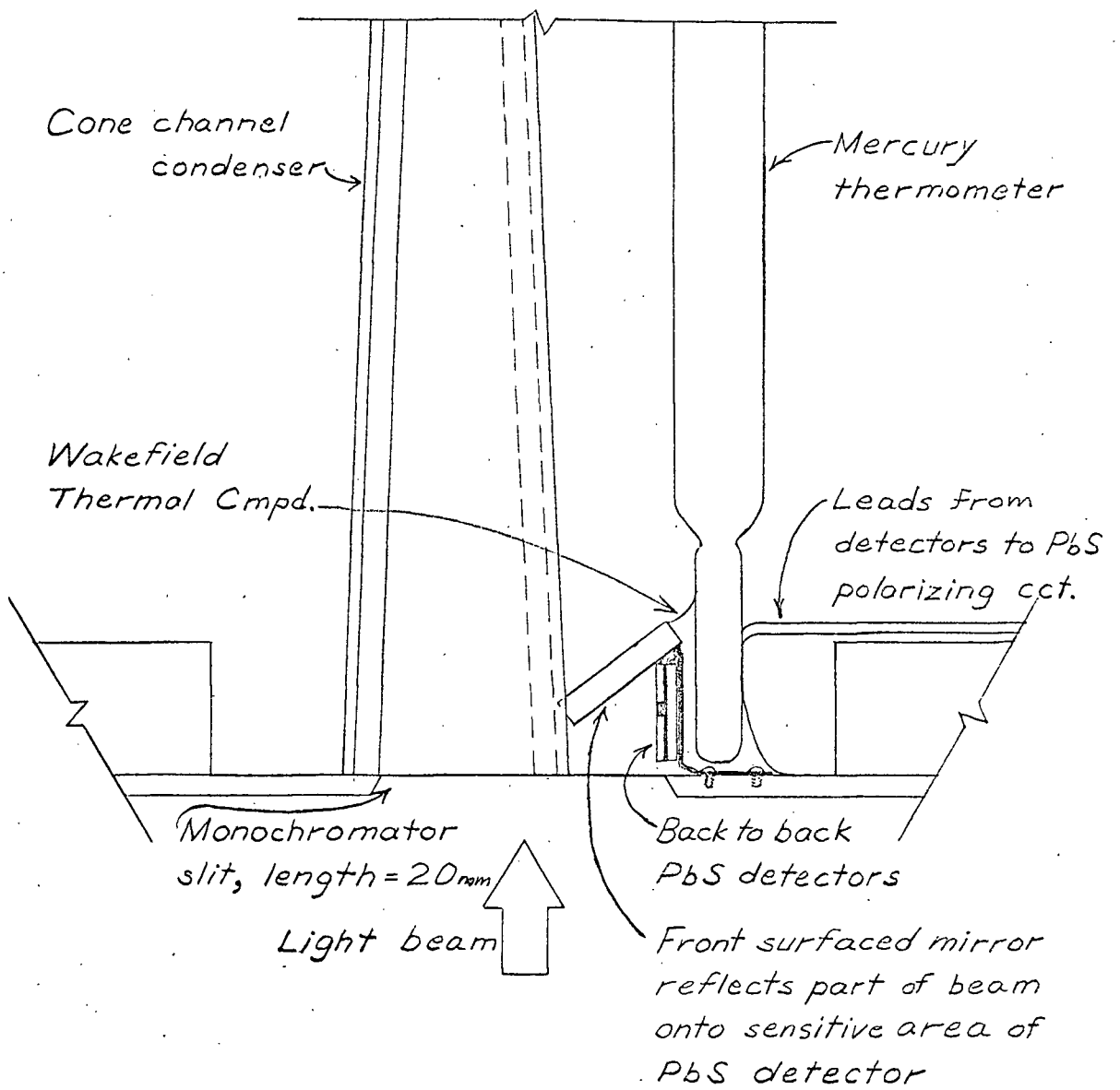Masked PbS cell used
as load resistor

FIGURE 4

PbS Detector: Mounting and Polarizing Circuit

intensity incident on the sample is lost. The masked PbS cell which acts as the load resistor is mounted back to back with the measuring detector, and is therefore in the same physical environment. Both cells are in thermal contact with the bulb of a mercury thermometer, the readings from which were used to correct all measurements to 24° C. The remaining circuitry necessary to operate the PbS cells as a detector is mounted in an electrically shielded box on top of the monochromator adjacent to the slit. Effective shielding of the detector and its leads was found to be very important for stable signal measurements.

3.2 Detection of the Lead Sulphide Cell Output

To determine the relative extinction coefficients by the action spectrum method, one must measure sets of light intensities throughout the spectrum. Since the intensities always enter the calculation as the ratio of one intensity to another, the electrical output of the PbS detector may be used in place of actual light intensities providing this output is a linear function of intensity over the range of wavelengths and intensities used. Because such a relationship was found to hold for the PbS detector used in the apparatus (see Section V - 1.21), only a stable measurement of the PbS signal is required.

The method of measurement is as follows. The monochromator light source is chopped at 235 Hz with a slotted wheel driven by a synchronous motor. Since the inherent frequency variation in the mains driving the motor is small, no stabilization is necessary. The amplifier in the detection network is only broadly tuned to the chopping frequency and is therefore insensitive to small changes in it.

The AC signal from the PbS cell inserted into the modulated

beam is AC coupled to the phase sensitive detector (hereafter referred to as the PSD) whose circuit is shown in Figure 5. The initial amplification is carried out by an active filter consisting of a Philbrick K2-W packaged amplifier with a Twin-T rejection filter in the feedback loop. The notch filter is designed with a low Q (Q = 6.2) to allow effectively constant amplification at 235 Hz since it was found the chopper wheel had a 3 Hz beat superimposed on its frequency output. The cause of the beat is obscure and is more easily allowed for electrically than corrected mechanically.

The reference voltage carries the phase information that determines how much of the signal amplitude appears as DC at the output of the PSD. When the signal and reference are precisely in phase, a complete half wave is detected, while if the two differ by a phase angle γ, the fraction of the signal amplitude detected is proportional to $\cos \gamma$. The reference voltage originates from a barrier layer cell onto which the beam from an automobile lamp falls. This beam is also chopped by the slotted wheel. The phase of the reference signal, relative to that from the PbS detector, is set by adjusting the azimuthal position of the barrier layer cell at the rim of the chopper wheel.

The output from the PSD is filtered through a 0.05 sec. time constant filter between the high and low terminals of a Keithley Model 150-A Microvoltmeter-Ammeter operated differentially. This filter stage cuts out the 60 Hz voltage between the circuit and chassis grounds of the microvoltmeter which are a design limitation of the instrument. The DC measurement is made potentiometrically, using the Keithley plus an Esterline-Angus Recording Milliammeter as the null detector. The bucking voltage is obtained from an external circuit. The potentiometric measurement

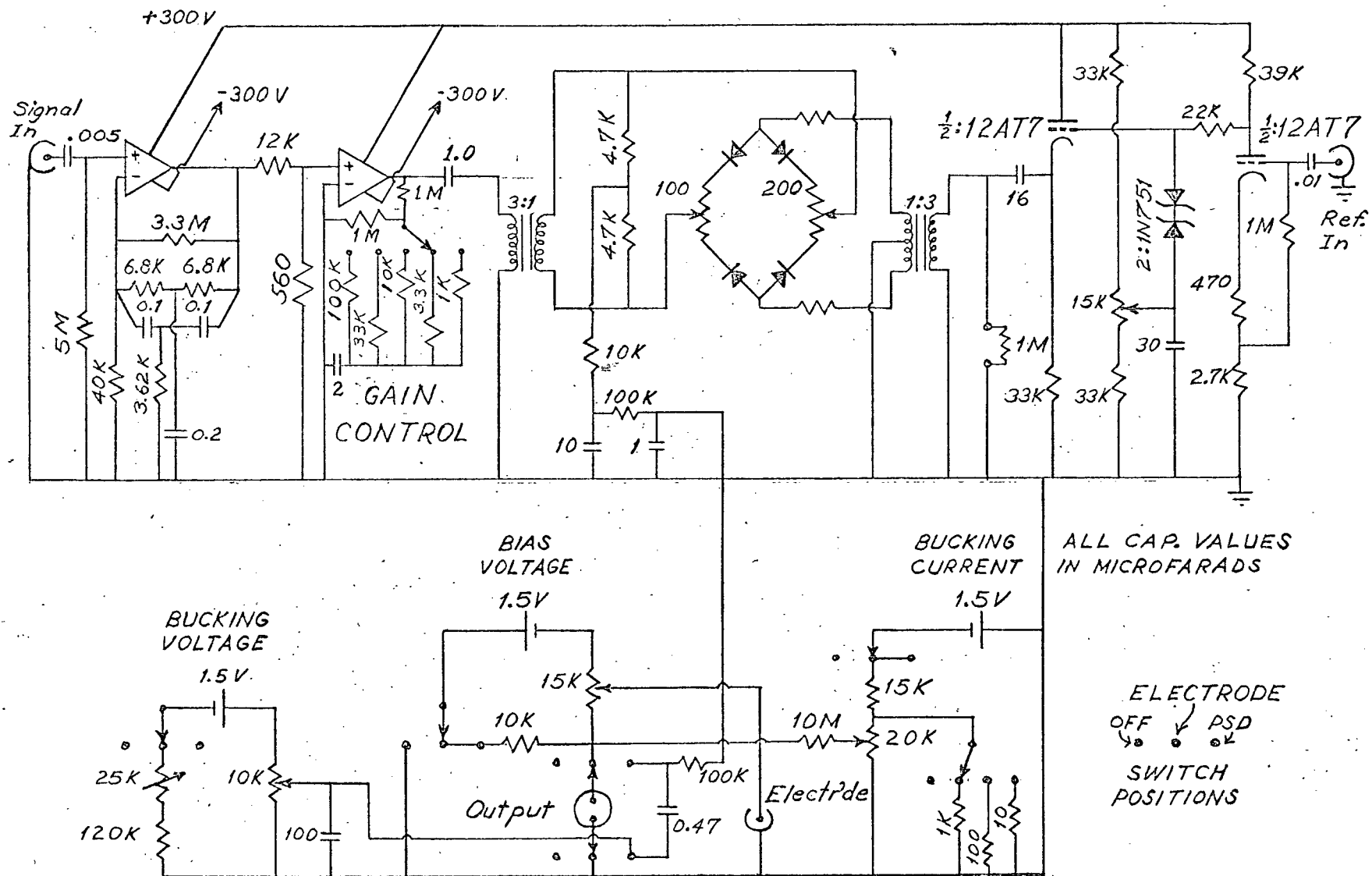## FIGURE 5
Circuit Diagram of Phase Sensitive Detector

has the advantages that expanded scales on both the microvoltmeter and the recorder may be used for more accurate measurements and that the measurement does not depend on the accuracy of the meter's calibration. The ultimate noise bandwidth of the PSD is then just the bandpass of the Esterline-Angus chart recorder, of the order of 0.5 Hz.

CHAPTER IV

Respiration Rate Sensor

IV-1. Principle of the Respiration Rate Sensor

The apparatus of Castor and Chance (4), on which the present instrument is based, was built to monitor the respiration rate of microorganisms in the presence of CO. Since their respiration is known to be inhibited by CO, and since the degree of inhibition decreases with increased intensity of illumination, it is possible to take an action spectrum of the relief of inhibition if one can obtain a convenient measure of the respiration rate.

A measure of this rate may be obtained using a polarized platinum electrode, which operates as follows. When Pt or Hg is polarized - 0.6 v to - 0.9 v with respect to a Ag + AgCl reference electrode, O_2 in a solution in contact with the cathode is electrolytically reduced, causing a current to flow in the external circuit. The reaction is generally specific for O_2 in this type of system since other ions which are easily reduced electrically in this voltage range, such as Ag^+, Cu^{++}, or Pb^{++}, are not normally used in biological media. Further, the reaction is pH independent, since H^+ reduction does not occur at polarizations under 1 volt (8).

Since the O_2 concentration at the Pt surface is zero, the rate of reduction, and therefore the electrical current, is dependent on the rate at which O_2 can diffuse to the electrode. This diffusion rate is directly proportional to the oxygen concentration in the solution.

When an electrode is placed in a drop, roughly of the same

diameter as the electrode, containing living cells, the opposing effects of respiratory uptake by the cells and diffusion of the oxygen in from the drop surface cause a steady state oxygen gradient to be set up. Changes in respiration cause changes in the steady state, which are measured as current changes in the electrode current.

IV-2. Electrode Chamber Design

The electrode chamber assembly is as shown in Figure 6. The needle of a hypodermic syringe was used both as a means of introducing the cell suspension to the tip of the Pt electrode, and as a base for the reference electrode. A 4 to 5 mm hollow silver needle was crimped to its tip and electroplated with AgCl to act as this reference. Other methods of mounting the silver were tried, but it was found any arrangement using solder slowly poisoned the cells, and caused the time over which they remained active to decrease to well under an hour.

When the apparatus is in operation, the drop of cell suspension is formed between the ground tip of the Pt electrode, the reference electrode, and the cover slip forming the bottom of the chamber.

IV-3. Electrode Setting

It was found empirically that the stability of the current depended both on the rate of O_2 uptake by the cells, and on the distance between the electrode and cover slip. Following Castor and Chance, it was found the best setting for the electrode separation was made by first measuring the current with the chamber filled with phosphate buffer, giving a current of the order of 6×10^{-8} amps. The electrode was then screwed down until the current in a drop of buffer was about 2.5×10^{-8} amps.

Copper wire welded to Pt

←Electrically grounded

Nut to adjust electrode level

2" diam. lucite rod→

Gas inlet at rear of chamber

Electrical conn. to ref. electrode clamped here

Brass collar sealed to glass O-ring seal

Gas out to 50 c.c. syringe

Spring

0.01" diam. Pt wire sealed into 2 mm glass rod

Drop of cell suspension

$\frac{5}{8}$" diam. hemispherical gas chamber

Syringe holding cell suspension

Glass cover slip

Setting screw to adjust chamber location

AgCl plated Ag tip acts as reference electrode

Aluminum collar supporting chamber
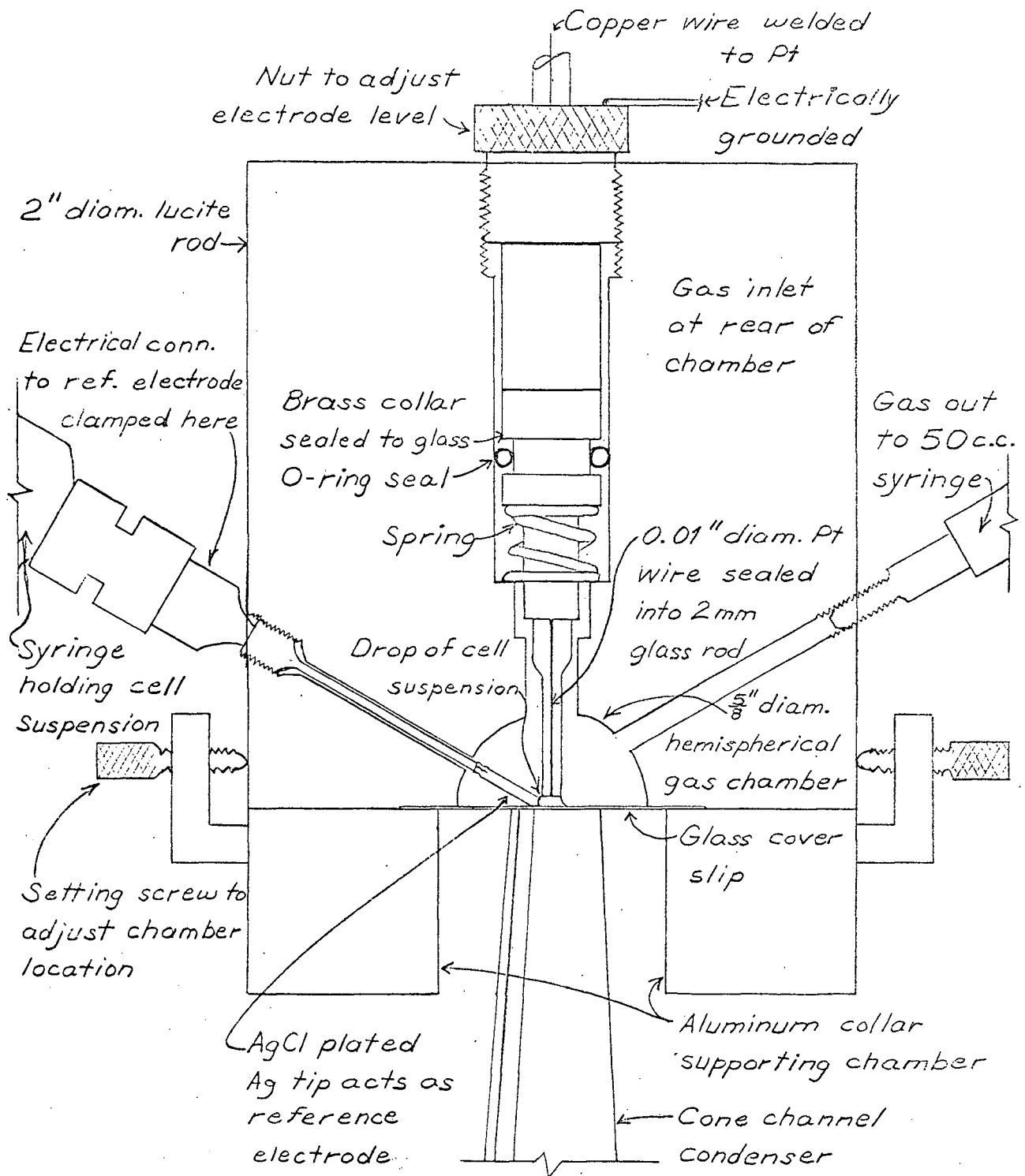
Cone channel Condenser

FIGURE 6
Electrode Chamber

This setting was retained when the drop of cell suspension was formed at the end of the electrode.

The cell concentration used was that concentration of respiring cells which would use up all the oxygen in the cell suspension sample in one minute. This time, called the respiration time, was determined by using a separate Pt electrode system set in a rotating sample holder. The cell suspension was diluted with phosphate buffer until a respiration time of the order of one minute was obtained. At this concentration, the cells remained active in the action spectrum apparatus for over two hours in most cases.

IV-4. Current Measurements

The current measurements were made by bucking out the electrode current with a variable opposing current. The bucking current was controlled by a ten turn helipot whose full scale deflection corresponded to between 100 na and 0.1 na on four succeeding decade ranges. The deviations from null as the steady state changed were observed on the Keithley 150-A Microvoltmeter-ammeter. When the ammeter is connected to the Esterline-Angus recorder, the smallest division on the chart represents 2×10^{-12} amps. The bias of the electrodes is set by another simple dry cell circuit controlled by a potentiometer. All this circuitry is housed in the cabinet with the phase sensitive detector and its associated amplifiers and transformers. The cable to the electrode is shielded, and the shield is grounded through the cabinet plug to the circuit ground of the phase sensitive detector. It is isolated, however, from the monochromator box, which is grounded through the shield on the cable from the PbS detector to the phase sensitive detector cabinet.

CHAPTER V

Calibration, Operation, and Performance of Apparatus

V-1. Calibration

1.1 Electrode

The Pt electrode was used only as the indicator of the balance between the photochemical effects of the monochromatic and comparison light beams. Thus, no calibration of the electrode current as a function of oxygen concentration was necessary for the operation of the apparatus. However, some parameters associated with the electrode's operation had to be determined.

The polarization voltage was determined by setting the Pt and Ag/AgCl electrodes in a 1 N NaCl solution in equilibrium with atmospheric oxygen. The Pt was made the cathode, the polarizing voltage was varied, and the current flowing in the external circuit plotted as a function of voltage. The resulting curve was sigmoid shaped under - 0.9 v, followed by a steep rise at voltages ($\geqslant$ 1.0 v) high enough to reduce the H^+ ions in solution. The polarization voltage was taken, from the top of the S, to be - 0.7 v, well below the H_2 producing potentials.

To check that the current was proportional to oxygen concentration, and not to some other substance in a buffer solution, the electrode current was measured as a function of oxygen concentration in a phosphate buffer solution 10^{-3} N in NaCl. The oxygen concentration was controlled by mixing varying quantities of the air equilibrated solution, in which the oxygen concentration should have been 20.9%, with a solution through which nitrogen had been bubbled to remove all dissolved oxygen.

The plot of current vs. dilution was approximately a straight line passing through the origin.

1.2 Lead Sulphide Detector

1.21 Intensity Response

The intensity of the monochromatic light was varied by inserting a number of clear glass slides into the incident beam in front of the entrance slit of the monochromator. The light was allowed to fall in turn on the lead sulphide cell, and on the sensitive element of an Eppley Thermopile in the same position. The lead sulphide cell was used with its incident light chopped at 235 Hz and the output detected on both an oscilloscope and the phase sensitive detector. The thermopile output for each intensity was taken as the average over ten measurements of the thermopile voltage change after a 30 second exposure to the unchopped light beam. These DC voltages were detected by the Keithley microvoltmeter and recorded on an Esterline-Angus recording milliammeter. In all cases, the reading error from the chart was of the same order of magnitude as the standard deviation in the voltage values.

It was found, as indicated in the Kodak Ektron Detector handbook, that the AC voltage change across the load resistor of the detection circuit was directly proportional to the light intensity. Further, the DC output of the PSD was also found to be directly proportional to the intensity. The voltages could thus be used in the calculation of the relative extinction coefficients.

1.22 Temperature Dependence of the Lead Sulphide Detector

As discussed in section III-2.23, the output of the lead sulphide detector, and therefore the phase sensitive detector, is temperature dependent, the variation of signal with temperature being given by

equation III-10. This expression was checked against a series of measurements on the PSD taken over the temperature range 24° C to 29° C. The inside mean value of the temperature coefficient, used as suggested by Wilson (9), was determined from these readings to be - 2.4×10^{-2} deg $^{-1}$ with a standard deviation of 0.2.

1.23 Absolute Calibration of the Detection System

While the output of the lead sulphide detector is directly proportional to the intensity at a given wavelength, the proportionality constant is somewhat wavelength dependent. To determine this dependence, and thus to allow the determination of the absolute light intensities causing a photochemical change, a further calibration was made. A series of intensity measurements were taken comparing the outputs of the thermopile and a lead sulphide cell. Readings were taken at 10 nm intervals between 365 nm and 1000 nm. Two layers of red cellophane were inserted in the beam for the readings between 750 nm and 1000 nm to remove the visible second order. The lead sulphide output was fed into the phase sensitive detector, and the DC output corrected for temperature deviations from 24° C. All voltages from the phase sensitive detector were recorded at the 10 X gain setting. The thermopile voltage changes were measured as described in Section 1.21 above. Table I contains the results of these readings.

1.24 Determination of Light Intensities Incident on the
Cell Suspension

In order to determine the light intensity incident on the sample, the ratio of the intensities at the top of the cone channel condenser, and at the lead sulphide detector beside the base of the cone had to be found. The ratio was expected to vary with wavelength, since it is

TABLE I

Comparison of P.S.D. and Thermopile Outputs

Note: (i) Polarization voltage of PbS pair = 15 v

(ii) Thermopile intensity calibration = 0.059 uv/uw/cm^2

Wavelength	P.S.D. Output in mV DC Corrected to 24° C and 10 X Gain	Thermopile Output in microvolts DC
Slit Width = 2.00 mm		
365	21.11 ± .19	0.80 ± .02
370	23.74 ± .18	0.88 ± .02
380	29.22 ± .17	1.04 ± .02
390	34.64 ± .21	1.31 ± .03
400	39.55 ± .15	1.60 ± .03
410	46.12 ± .15	1.96 ± .03
420	53.19 ± .15	2.32 ± .04
430	60.66 ± .15	2.60 ± .04
440	67.73 ± .15	2.90 ± .06
450	75.38 ± .15	3.32 ± .06
Slit Width = 1.515 mm		
450	41.72 ± .17	1.95 ± .06
460	48.07 ± .17	2.23 ± .06
470	53.97 ± .17	2.50 ± .06
480	57.39 ± .19	2.65 ± .06
490	61.43 ± .20	2.83 ± .06
500	65.05 ± .21	3.02 ± .06
510	70.00 ± .21	3.28 ± .06
520	78.38 ± .21	3.70 ± .06
530	82.48 ± .21	3.85 ± .06
540	84.38 ± .21	3.96 ± .06
550	86.83 ± .21	4.06 ± .06
560	89.48 ± .21	4.17 ± .06
570	92.23 ± .21	4.31 ± .06
580	94.60 ± .22	4.37 ± .06
590	96.80 ± .22	4.54 ± .06
600	98.70 ± .22	4.63 ± .06

Wavelength	P.S.D. Output in mV DC Corrected to 24° C and 10 X Gain	Thermopile Output in microvolts DC
Slit Width = 1.00 mm		
600	40.38 ± .15	1.61 ± .02
610	41.28 ± .15	1.61 ± .02
620	42.40 ± .16	1.65 ± .02
630	42.75 ± .16	1.65 ± .02
640	48.42 ± .17	1.83 ± .02
650	50.67 ± .17	1.92 ± .02
660	49.82 ± .17	1.86 ± .03
670	49.22 ± .17	1.79 ± .03
680	48.87 ± .17	1.76 ± .03
690	48.64 ± .18	1.72 ± .03
700	48.14 ± .18	1.69 ± .03
710	46.49 ± .18	1.62 ± .03
715	49.49 ± .18	1.71 ± .03
720	54.24 ± .18	1.89 ± .03
730	57.44 ± .18	1.96 ± .03
740	55.44 ± .18	1.89 ± .03
750	53.74 ± .18	1.80 ± .03
Slit Width = 1.00 mm **Two layers red cellophane in optical path**		
750	28.48 ± .1	1.06 ± .02
760	27.80 ± .1	1.01 ± .02
770	27.35 ± .1	0.98 ± .02
780	26.8 ± .1	0.96 ± .02
790	26.4 ± .1	0.96 ± .02
800	25.94 ± .1	0.89 ± .02
810	25.64 ± .12	0.89 ± .02
820	25.44 ± .12	0.86 ± .02
830	25.36 ± .12	0.83 ± .02
840	25.48 ± .12	0.85 ± .02
850	25.83 ± .12	0.87 ± .02
860	26.39 ± .12	0.88 ± .02
870	27.40 ± .16	0.90 ± .02
880	28.27 ± .17	0.90 ± .02
890	29.07 ± .17	0.93 ± .02
900	29.82 ± .17	0.93 ± .02
910	30.57 ± .17	0.96 ± .02
920	31.22 ± .17	1.00 ± .02
930	31.54 ± .16	0.98 ± .02
940	31.90 ± .16	1.01 ± .02
950	32.17 ± .16	1.01 ± .02
960	32.44 ± .16	0.98 ± .02
970	32.65 ± .16	1.01 ± .02
980	32.73 ± .16	1.03 ± .03
990	32.73 ± .16	1.02 ± .02
1000	32.66 ± .16	0.99 ± .02

a measure both of the effect of the cone on the spectral intensity, and the ability of the grating to fill the slit uniformly over the range of wavelengths used.

The signals from lead sulphide detectors mounted both permanently at the base of the cone, and directly on its end, were measured sequentially on the phase sensitive detector. The detector on the end of the cone was fixed in the position which gave the maximum output, and was separated from the cone only by a glass cover slip. Measurements were made in chopped light from 300 nm to 1000 nm, (a red filter was placed in the beam from 700 nm to 1000 nm to remove the second order overlap). The phase sensitive detector readings were all corrected to 24° C and an amplifier gain setting of 100 X. The results, expressed as the ratio, St/Sb, of the corrected signal at the top of the cone, to that at the bottom, are displayed in Figure 7.

V-2. Determination of the Action Spectrum

2.1 Preparation of the Biological Sample

The cell suspension used here to test the apparatus was Bakers yeast. It was maintained for two weeks in 0.15 M phosphate buffer solution, 1% to 2% ethanol by volume, at pH 6.5 to 7.5. The suspension was continuously bubbled with filtered air. Sterile procedures were not followed, and the yeast was left exposed to the air throughout the experimental period. When required for an experiment, a sample of the suspension was made 10^{-3} N in NaCl during dilution to a cell concentration which gave a respiration time of 1 min.

2.2 Operating Procedure

The procedure for the operation of the action spectrum apparatus is as follows:

(i)   The electronics are allowed to warm up for at least an hour before any measurements are attempted.

(ii)   The position of the electrode chamber relative to the cone channel condenser is adjusted with setting screws until the electrode is centered directly over the center of the end of the cone. The correct position may be found by looking up through the cone from inside the monochromator with the aid of a mirror. The Pt wire in the end of the glass electrode is seen as a small bright dot in the multiple reflections in the cone's walls. The center position is easily determined by watching the multiple patterns vary in symmetry as the electrode is shifted.

(iii)   The phase sensitive detector output is maximized by:

(a) Setting the reference signal to a symmetrical square wave, as seen on an oscilloscope.

(b) Adjusting the phase of the reference signal with respect to the PbS cell signal to give the maximum DC output. This is conveniently done by changing the azimuthal position of the barrier layer cell from which the reference signal originates.

(iv)   The entrance and exit slits are set for the desired bandpass.

(v)   The electrode chamber is filled with a gas mixture, saturated with water vapour to prevent evaporation of the

drop, of 4 parts CO to 1 part O_2.

(vi)   With the electrode spacing set as in Section IV-3, the
exit slit fishtail closed, and the chopper wheel turned off,
a drop of cell suspension is introduced between the Pt and
reference electrodes. The drop, held by surface tension
between the two electrodes and the cover slip, should be
roughly of the same diameter as the tip of the glass-sealed
Pt electrode. The drop of cells is allowed to attain a
steady state of respiration, as indicated by a reasonably
stable electrode current. This takes 15 to 20 min., and the
current is usually between 5 and 50 na for yeast.

(vii) The monochromator is set to 550 nm and the exit
slit fishtail opened. The electrode current should decrease
because the light, by reducing the inhibition by CO, speeds
up the respiration. For yeast suspensions, the decrease
was always about 1 to 2 na.

(viii) The comparison beam is switched onto the sample,
and its intensity altered until the two beams produce the
same steady state electrode current.

(ix)   When balance is obtained the light chopper is
switched on, the intensities of the monochromatic and
reference beams measured on the phase sensitive detector,
and the temperature at the lead sulphide detector recorded.

(x)   The wavelength is varied and the measurements
repeated as long as the cells remain active enough to keep
the electrode current stable, usually about two hours or

more. If it is necessary to change gain settings on the
phase sensitive detector during the course of the experi-
ment, the gain ratio should be determined, since in the
present apparatus the gain seems to depend somewhat on the
external conditions.

(xi)   When the experiment is completed, the chamber is
flushed several times with water, then left filled with
distilled water, to prevent the Ag/AgCl reference electrode
from deteriorating.

2.3 Calculation of Relative Extinction Coefficients

With the data obtained from the preceeding procedure, the
relative extinction coefficients of the terminal oxidase of the cells under
examination may be determined as follows:

(i)   The phase sensitive detector readings from the
monochromatic and comparison beams are corrected for
temperature dependence to the standard value of 24° C.

(ii)   The temperature corrected voltages corresponding
to the monochromatic light intensities at the base of the
cone are adjusted to give the intensities incident on the
sample. Figure 7 gives the factor, St/Sb, by which the
intensity at each wavelength must be multiplied to give the
final value W_λ . In general, these figures should in turn
be multiplied by the ratio of the thermopile readings to
those of the lead sulphide detector, as determined in
Section V-1.23. However, the ratio is a slowly varying
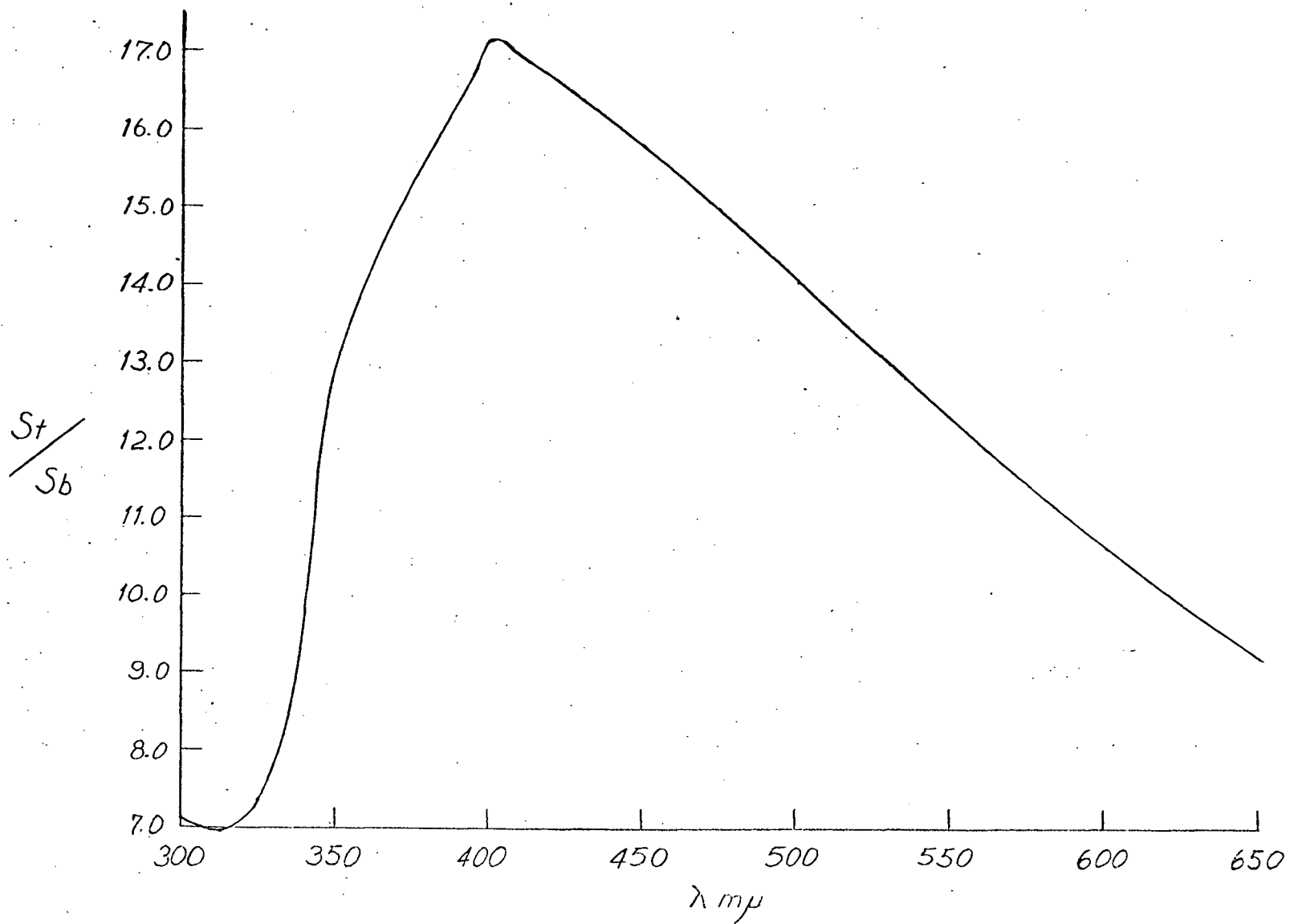function of wavelength, varying only because the detectivity

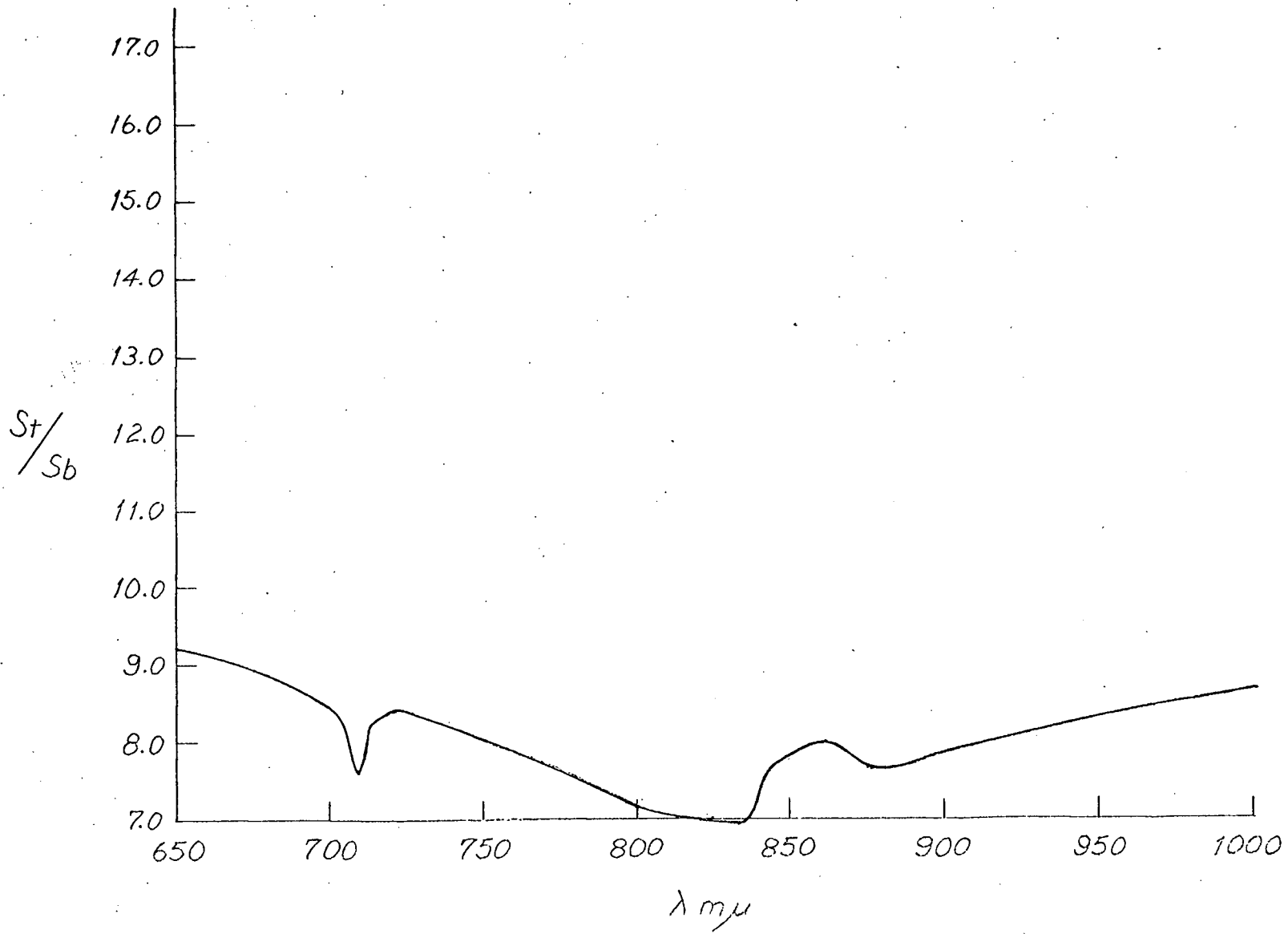*FIGURE 7*

St/Sb Calibration Curve

FIGURE 7 (cont'd)

St/Sb Calibration Curve

of the lead sulphide cell increases in the infra-red. Over the wavelength interval used in the present experiment, the ratio fluctuates about the mean with a standard deviation of less than 1%, so no such factor is used in the calculation. Also, it is not necessary to make either an St/Sb, or a thermopile adjustment to the voltages associated with the comparison beam. It is of fixed wavelength, and therefore both numerical factors cancel out in the computation of the relative extinction coefficients.

(iii) The ratio of the extinction coefficients at some wavelength λ , to that at 550 nm, is calculated from:

$$\frac{\epsilon_\lambda}{\epsilon_{550}} = \frac{C_\lambda \; W_{550} \; 550}{W_\lambda \; C_{550} \; \lambda} \qquad (I\text{-}8)$$

V-3. Performance

3.1 Action Spectrum of Yeast

The action spectrum of the terminal oxidase of Bakers yeast, as determined by the above method, is illustrated in Figure 8. The location of the peaks coincides with the peaks of the absorption spectrum of cytochrome a-a_3, and thus identifies cytochrome as the terminal oxidase.

3.2 Accuracy of the Action Spectrum Determination

The limit of accuracy with which any calculated point of the action spectrum may be determined is the sum of the inherent errors and uncertainties in each of the terms in equation I-8:

(i) Uncertainties in W_λ :

(a) Both the random error, and the reading error from the chart introduced less than 1% error in W_λ and were neglected.

Note: × ⇒ Data of Castor and Chance
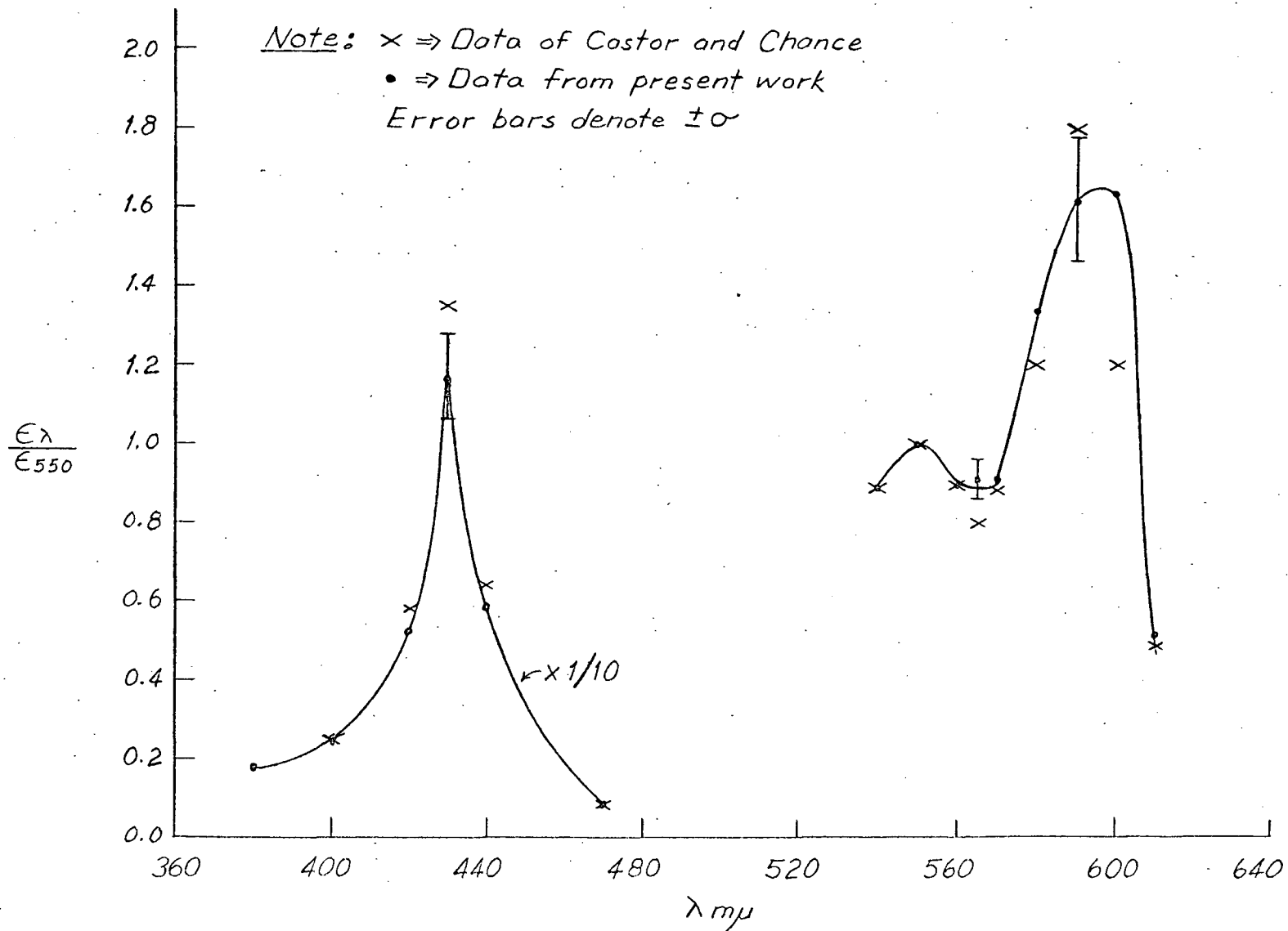 • ⇒ Data from present work
  Error bars denote ±σ

←×1/10

λ mμ

FIGURE 8

Action Spectrum of the CO Inhibition of Respiration in Baker's Yeast

(b) The calculation of the temperature coefficient
and its application to the PSD output introduces
a 1% uncertainty in the monochromatic intensities,
and a negligible uncertainty in the comparison
intensities, as shown below:

A temperature corrected voltage from the PSD is
determined from the expression

$$\log S_f = \log S_i + \alpha \Delta T$$

where S_f = signal corrected to 24° C

S_i = signal at a temperature differing from

24° C by ΔT

Thus, the actual error in $\log S_f$, $\Delta(\log S_f)$,
will be the sum of the actual errors in $\log S_i$,
and $\alpha \Delta T$. The error in $\log S_i$, $\Delta(\log S_i)$,
is found by differentiation to be

$$\Delta(\log S_i) = \frac{\Delta S_i}{S_i}$$

where ΔS_i is the uncertainty in S_i due to
randomness and reading errors. Since α is taken
to be known to $\pm 0.1^\circ$ C, the uncertainty in $\alpha \Delta T$
will be:

$$\left(.02 + \frac{.1}{\Delta T}\right) \alpha \Delta T$$

Thus:
$$\Delta(\log S_f) = \frac{\Delta S_i}{S_i} + \left(.02 + \frac{.1}{\Delta T}\right) \alpha \Delta T$$

The uncertainty in the final value S_f, will then

be
$$\Delta S_f = \Delta(\log S_f) \times S_f$$

or, expressed as a percentage

$$\frac{100 \times \Delta S_f}{S_f} = \Delta(\log S_f) \times 100$$

$$= \left[\frac{\Delta S_i}{S_i} + \left(.02 + \frac{.1}{\Delta T}\right) \alpha \Delta T\right] \times 100$$

So, for a typical temperature correction of the signal corresponding to a monochromatic beam:

$$\Delta T = 2 \ C^o \qquad S_i = 0.1 \ mv$$

$$S_i = 20 \ mv \qquad \alpha = 2.3 \times 10^{-2}$$

These figures give the uncertainty in the corrected voltage as approximately $\pm$ 1%, and applying figures for the comparison beam intensities gives a possible error much less than 1%.

(c) Due to a variation in the gain levels of the PSD, the values of St/Sb are only reproducible to $\pm$ 5%, introducing this further error into W_λ . This error is not inherent to the method, however, and can probably be removed (see Chapter VI).

(d) The balance point, at which the photochemical effects of the monochromatic and comparison lights are the same is found by equalizing the slopes of the recorded current output under the two illuminations. The estimation limits the determination of the balance point to within $\pm$ 1%. Since such a balance is required twice for any point on the action spectrum, a $\pm$ 2% error could be introduced in this way.

(e) The error in the ratio $550/\lambda$ is negligible.

Thus, the accuracy of the ratio $\epsilon_\lambda / \epsilon_{550}$ is found to be:

$$\frac{\epsilon_\lambda}{\epsilon_{550}} = \left[\frac{C_\lambda}{W_\lambda \pm 6\%} \frac{W_{550} \pm 6\%}{C_{550}} \frac{550}{\lambda} \right] \pm 2\%$$

$\epsilon_\lambda / \epsilon_{550}$ is only sure, then, to within $\pm 14\%$.

CHAPTER VI

Suggested Improvements

VI-1. Reduction of Error in Present Apparatus

Considerable improvement in the accuracy of the instrument, without drastic alterations, can be obtained in the following ways:

(i)   Removing the uncertainty in the gain of the amplifier when the ranges are changed, or altering the gain ratios so that all measurements could be taken on one setting, should reduce the error in St/Sb to 1 or 2%.

(ii)   Changing the system of introducing filters when the beams are switched should remove the transient effects on the drop, and eliminate the uncertainty in the balance point determination. These improvements should reduce the limits of accuracy to $\pm$ 6% for the action spectrum of any given biological sample.

VI-2. Alterations to Increase Range and Sensitivity of Apparatus

The following are a few suggestions related to possible extensions of the apparatus, both in accuracy and range.

(i)   Air condition the room in which the apparatus is located to control temperature variations. If these variations could be reduced to $\pm$ 0.5° C or less, then (ii) below would not be needed.

(ii)   Make the output of the lead sulphide cell independent of temperature by adding a temperature controlled compensating circuit element to the detector's voltage supply.

One such method would be to put a thermistor of appropriate

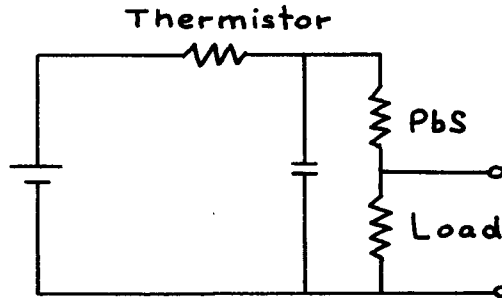size in series with the supply battery, as shown below.

Figure 9

Thermistor Controlled Circuit for PbS Polarization

If the thermal characteristics of the thermistor and

detector are similar over the normal range of room tempera-

tures, the measurements of light intensity should be in-

dependent of temperature.

(iii) Replace the present system for introducing the

comparison light with a beam from a separate bulb outside

the box. All filters and the intensity control could go

into the comparison beam outside the monochromator. The

beam could enter the monochromator with the beam axis

parallel to, but just below, the exit slit. The beams

could then be interchanged by sliding in a small mirror

to deflect this beam onto the slit and at the same time cut

off the monochromatic beam. The slit would thus be filled

with light at all times.

Such a change would necessitate changing the method of chopping the light. A possible and better method would be to have the detector mounted on one prong of a magnetically driven tuning fork (Bulova Watch Co.). Such devices are available with vibration amplitudes of sufficient magnitude to switch the sensitive area in and out of the light, if masks are employed. The fork could be mounted beside the base of the cone, in the same optical location as the present detection system. The light chopping wheel could then be discarded from the system entirely. The reference signal for phase sensitive detection could be taken from the other half of the fork, using it as a mechanical chopper in a circuit. The above outlined arrangement would have several advantages over the present system:

(a) Virtually no scattered light would be introduced into the optical path by reflection from the filters and intensity controlling louvers. While not significant at the intensities and wavelengths used in the initial testing of the apparatus, the scattered light is of appreciable intensity, as observed by the unaided eye, and could become important at shorter wavelengths where the available intensity is low.

(b) Since the exit slit would be filled with light throughout the transition between beams, the drop

would be fully illuminated at all times, and no transient effects would appear. This would greatly increase the speed at which the action spectrum could be taken.

(c) Elimination of the chopping wheel would allow uninterrupted illumination of the sample throughout the intensity measurements.

(iv)   The ultra-violet range of the instrument could be extended by using a hydrogen lamp as the source in the shorter wavelength region. A combined u.v.-visible source could be obtained by mounting the tungsten lamp in the usual way, and mounting a hydrogen lamp directed at 90° to be optical path of the incandescent light. A dichroic mirror placed at the intersection of the two light beams, at 45° to each of them, would reflect the u.v. light from the hydrogen lamp into the monochromator while allowing the visible light from the tungsten lamp to pass straight through unreflected. Such filters are available which will reflect greater than 90% of the u.v. while passing more than 90% of the intensity of the visible light.

BIBLIOGRAPHY

1. Setlow, R.B. and Pollard, E.C., "Molecular Biophysics" Addison-Wesley Publishing Co., Inc. (1962) pp. 267-305.

2. Horio, T. and Taylor, C.P.S.; J. Biol. Chem. 240: 1772 (1965).

3. Warburg, O., "Heavy Metal Prosthetic Groups and Enzyme Action", Oxford University Press (1949).

4. Castor, L.N. and Chance, B.; J. Biol. Chem. 217: 453 (1955).

5. Bucher, T. and Kaspars, J.; Biochim et Biophys. Acta, 1: 21 (1947).

6. Williamson, D.E.; J. Opt. Soc. Amer. 42: 712 (1952).

7. Jones, R.C., in "Advances in Electronics" Vol. V, L. Morton, Editor; Academic Press Inc. (1953).

8. Davies, P.W., in "Physical Techniques in Biological Research" Vol. IV, W. Nastuck, Editor; Academic Press Inc. (1962).

9. Wilson, E.B., Jr. "An Introduction to Scientific Research" McGraw-Hill Book Co. Ltd. (1952) pp. 232-276.